applied sciences

MDPI

Article

Investigation of Innovative High-Response Piezoelectric Actuator Used as Smart Actuator–Sensor System

Marko Šimic * and Niko Herakovič

Faculty of Mechanical Engineering, University of Ljubljana, 1000 Ljubljana, Slovenia; niko.herakovic@fs.uni-lj.si
* Correspondence: marko.simic@fs.uni-lj.si; Tel.: +386-1-4771-797

Abstract: This paper presents an experimental analysis of a high-response piezoelectric actuator system for the modular design of hydraulic digital fluid control units. It focuses on determining static and dynamic characteristics, forming the basis for developing a smart Industry 4.0 component that incorporates both actuator and sensor function. The design process examines the main challenges, advantages, disadvantages, and working principles to define parameters that impact the actuator's behaviour and performance. The new piezoelectric actuator system features three piezoelectric stack actuators in series, enabling simultaneous actuation and sensing by applying and measuring the electrical voltage at each piezo element. The experimental setup and test methodology are explained in detail, revealing that the new design, combined with an appropriate open-loop or closed-loop control method, offers superior actuator stroke control, high stroke resolution, and a high-dynamic step response. This paper proposes a concept of a smart piezo actuator system focused on I4.0 and an actuator administration shell, integrated with 5G and RFID technology, which will allow automatic plug-and-play functionality and efficient interconnection, communication, and data transfer between the hydraulic valve and the piezoelectric actuator system.

Keywords: piezoelectric actuator; experimental analysis; static characteristics; dynamic characteristics

check for updates

Citation: Šimic, M.; Herakovič, N. Investigation of Innovative High-Response Piezoelectric Actuator Used as Smart Actuator–Sensor System. *Appl. Sci.* **2024**, *14*, 8523. https://doi.org/10.3390/app14188523

Academic Editors: Vito Tič and Darko Lovrec

Received: 20 August 2024
Revised: 17 September 2024
Accepted: 18 September 2024
Published: 22 September 2024

Copyright: © 2024 by the authors. Licensee MDPI, Basel, Switzerland. This article is an open access article distributed under the terms and conditions of the Creative Commons Attribution (CC BY) license (https://creativecommons.org/licenses/by/4.0/).

1. Introduction

The concept of future factories demands new designs and developments of sustainable, energy-efficient, and intelligent hydraulic systems and components. Industry 4.0, along with key enablers such as the Industrial Internet of Things (IIoT), standardized communication protocols (e.g., OPC-UA), new data transfer methods, and AI-based approaches, as well as facilitated efficient data gathering, transfer, and analytics [1]. Conversely, factories of the future rely on various approaches such as modular design with plug-and-play capabilities, distributed systems with integrated local intelligence, 5G and edge computing, cyber-physical systems (CPSs), and data-driven digital twins, among others [2]. In these intelligent systems and components, self-awareness, health monitoring, and predictive maintenance are incorporated. To successfully digitize a system or component and effectively monitor or evaluate its behaviour, key characteristics must be defined, stored in local clouds, and made available for further use and services. This paper focuses on the design of a new actuator system integrated into a hydraulic on/off valve, which is used in hydraulic digital fluid control units (DFCUs), and its representation of static and dynamic performance. Digital hydraulics and DFCUs constructed from on/off valves offer several advantages over conventional hydraulics and sliding spool valves, including a higher power density, precise control, greater force output, and improved energy efficiency [3]. Furthermore, digital hydraulics combined with a piezoelectric actuator system has the potential to significantly improve electrical energy efficiency, as well as enhance the static and dynamic performance of hydraulic valves, such as DFCUs [4]. The most commonly used actuators in conventional hydraulics are electromagnetic actuators (solenoids), which are robust and reasonably priced. However, their performance is limited when switchover

times below 1 ms are required, a key factor for DFCUs in high-dynamic and high-precision hydraulic linear drives. As noted by the authors in [3], some commercially available on/off valves used in digital fluid power systems have response times ranging from 3 to 10 ms. Shorter switchover and response times are hindered by magnetic induction and eddy currents when switching the electrical current on. Differences in the static and especially the dynamic characteristics of any type of hydraulic valve, when combined with a control method, have a significant impact on hydraulic linear drive behaviour, including stroke resolution, precise uniform motion, step response, and operational stability [5].

By using alternative actuators, particularly piezoelectric actuators, which offer the best practical potential, significantly shorter response times and a lower electrical energy consumption can be achieved, especially in the steady active state [6–9]. On the one hand, the switchover times of electromagnetic actuators range between 10 and 20 ms, while on the other hand, piezoelectric actuators can achieve switchover times of less than 1 ms. In addition to these advantages, piezoelectric actuators offer high precision, flexible stroke control, immunity to electromagnetic interference, and structural scalability [10].

This paper begins by presenting the theoretical background of piezoelectric actuators and piezoelectricity, explaining both the direct and inverse piezoelectric effects, along with the core concept of the actuator–sensor approach. The following section focuses on the design and functionality of the piezoelectric actuator system, followed by a detailed explanation of the experimental methodology. The main part of the paper presents the experimental characterization of the static and dynamic performance of the piezoelectric actuator system, which serves as the foundation for developing a smart actuator system concept. The proposed actuator administration shell concept will be used in the future development of a real actuator–sensor system, as well as switching valves and DFCUs.

2. Theoretical Background of Piezoelectric Actuators

Piezoelectric materials can be utilized in both sensor and actuator technologies. When pressure is applied to piezoelectric materials such as quartz crystals, an electric potential is generated; this phenomenon is known as the piezoelectric effect and is employed in sensor technologies. Conversely, piezoelectric actuators operate based on the inverse piezoelectric effect. In this process, applying an electrical potential to the piezoelectric material causes a change in its shape, specifically an extension in the direction of the material polarization [11].

A detailed background on the practical use and functionality of piezoelectric actuators is provided in [12,13], where authors focus on the potential applications of piezoelectric actuators and usage in various types of hydraulic valves, including conventional hydraulics and pneumatics, as well as in high-response continuously operated spool valves. In this paper, we focus only on the essential piezoelectric characteristics and operational principles to highlight the key parameters of piezoelectric actuators that significantly impact the static and dynamic performance of the new piezoelectric actuator system.

Linear multilayer piezoelectric stack actuators, as shown in Figure 1a, are suitable for hydraulic valves, including DFCUs. The image depicts a 32.4 mm long piezo stack with a 7×7 mm cross-sectional area. It has two electrical connections; the blue one represents the negative pole, while the red one represents the positive pole [14]. In our application, we use an electrical voltage ranging from 0 V to 200 V. Figure 1b illustrates a schematic representation of a multilayer piezoelectric stack actuator. In this figure, l represents the initial height, h denotes the thickness of the PZT layer, P stands for the polarization of the piezo ceramic material, and Δl indicates the extension of the piezo stack when electrical voltage is applied (active state). F represents the generated force, while U refers to the applied electrical voltage, with positive and negative poles. The main properties for selecting a piezoelectric actuator (PZT) or piezo element (PE) for a particular application are as follows: (1) dimension (cross-section, length, or height l), (2) force generation (F), (3) extension (Δl), and (4) response time. Piezoelectric stack actuators consist of several piezoceramic plates with thickness h, as shown schematically in Figure 1b. An advantage

of these multilayer stack actuators is that they require a lower supply voltage (up to 200 V), which is important for applications in fluid power technology and assembly automation where a high response, energy efficiency, and a high stroke resolution are crucial. These actuators can generate high forces up to several kN (e.g., the piezo stack shown in Figure 1a generates 2 kN) but have small extensions up to 0.15% of the actuator's length or height.

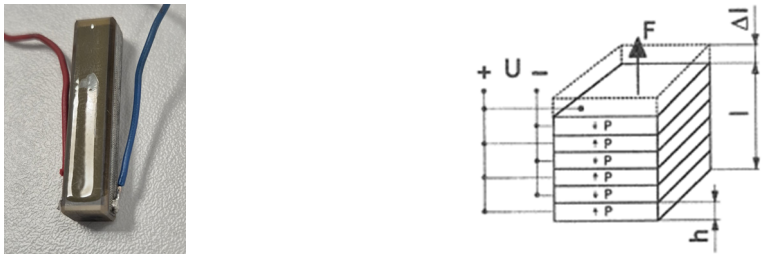

(**a**) (**b**)

Figure 1. Real picture of linear multilayer piezoelectric stack actuator (**a**) and operational principles (**b**).

The fundamentals of piezoelectric actuators and the simplified mathematical formulations described in this paper are derived from several sources [15,16]. A piezoelectric actuator is characterized by its force–displacement curve and the electrical charge versus electrical voltage curve. Figure 2 illustrates the force–displacement characteristic curve for a piezoelectric stack actuator, which describes its mechanical performance. This performance can be expressed using a basic mathematical formula that defines the electro-mechanical relationship as presented in [15,16]. The characteristic curve defines the operating point of the piezoelectric stack actuator (OP) under specific loading conditions. Equation (1) represents the displacement x_{pzt} of the piezoelectric stack actuator. In this paper, we focus only on Equation (1) and its associated characteristic curve, while the electrical charge versus electrical voltage curve is discussed in detail in [15,16]. This curve is crucial for understanding the charging of the piezoelectric stack actuator with a typical electrical capacitance C. The variables in Equation (1) are as follows: x_0 is the stress-free displacement [m/V], U_{pzt} is the supply voltage [V], k_{pzt} is stiffness [N/m], and F_{pzt} is the generated force [N]. It is important to note that the performance of piezoelectric actuators depends on the piezoelectric material used and the effective stiffness, as highlighted in [17]. Additionally, the characteristics of piezoelectric stacks can vary under different working conditions, such as temperature and the type of AC or DC signal used for testing, as explained in [18].

$$x_{pzt} = x_0 \cdot U_{pzt} - \frac{1}{k_{pzt}} \cdot F_{pzt} \tag{1}$$

Under no-load conditions, the piezoelectric stack actuator does not exert any force, and its displacement x_{pzt} corresponds to the free displacement x_{free}. The free displacement varies linearly with the applied electrical voltage U_{pzt} (illustrated in Figure 2 as examples U1, U2, and Umax) and is defined by Equation (2). When the piezoelectric stack actuator operates under a very large load (exceeding the generated force), its output displacement x_{pzt} becomes zero, and the actuator generates a blocking force F_{block}, as described by Equation (3). Additionally, when the piezoelectric stack actuator operates at the maximum voltage U_{max}, Equation (1) can be rearranged into the form presented in Equation (4), where the generated force is reduced by a portion of the actuator's displacement [15,16].

$$x_{free} = x_0 \cdot U_{pzt} \tag{2}$$

$$F_{block} = k_{pzt} \cdot x_0 \cdot U_{pzt} \tag{3}$$

$$F_{pzt} = -k_{pzt} \cdot x_{pzt} + k_{pzt} \cdot x_0 \cdot U_{\mathrm{max}} \tag{4}$$

A key consideration when using a piezoelectric stack actuator in practical applications is the type of preload applied to the actuator. As detailed in [15,16], a piezoelectric actuator behaves as an elastic body with a specific stiffness, denoted as k_{pzt}. Mechanically, it can be subjected to two distinct types of loading: the first is when the load remains constant during the extension (displacement) process and the second is when the load on the piezo stack varies during the extension process. In our investigation, we focus on the second scenario. Figure 3 illustrates the piezoelectric stack actuator loaded with a spring of stiffness k_s.

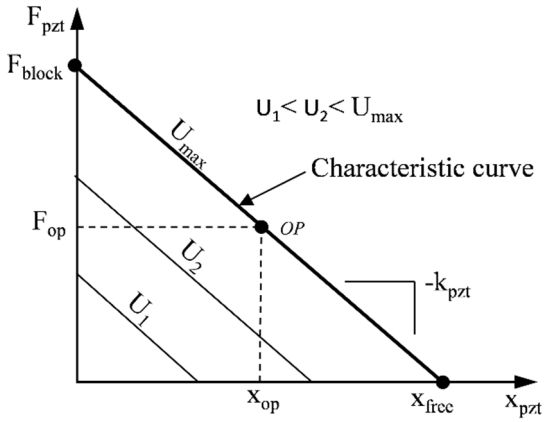

Figure 2. Force–displacement curve for a piezoelectric stack actuator.

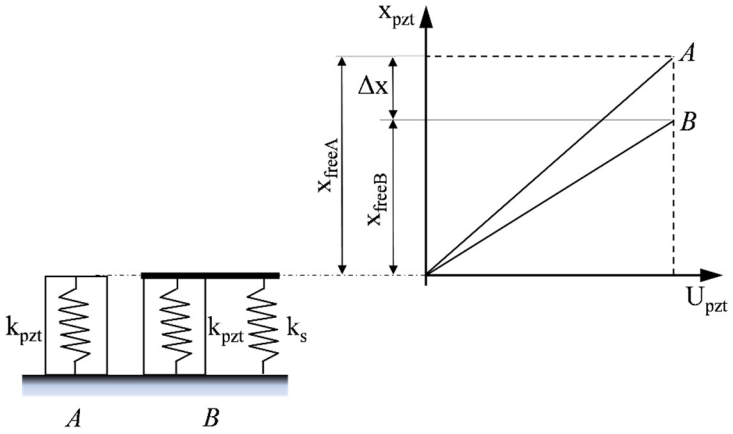

Figure 3. Effect of a spring preload on a piezoelectric stack actuator.

The free displacement of the unloaded piezoelectric stack actuator is given by the simplified Equation (5) (case A), where F_{pzt} represents the generated force of the piezoelectric stack actuator and k_{pzt} denotes its stiffness. The free displacement of the spring-loaded piezoelectric stack actuator (case B) is described by Equation (6). A spring load affects the free displacement capability of the piezo stack, reducing it by Δx, as shown in Equation (7). Furthermore, the free displacement of the loaded piezoelectric stack actuator is expressed as a function of the original free displacement, as described in Equation (8) [11,15].

$$x_{freeA} = \frac{F_{pzt}}{k_{pzt}} \tag{5}$$

$$x_{freeB} = \frac{F_{pzt}}{k_{pzt} + k_s} \tag{6}$$

$$\Delta x = x_{freeA} \cdot \left(1 - \frac{k_{pzt}}{k_{pzt} + k_s}\right) \tag{7}$$

$$x_{freeB} = \frac{k_{pzt}}{(k_{pzt} + k_s)} \cdot x_{freeA} \quad (8)$$

3. Piezoelectric Actuator System Design

The main idea of the piezoelectric actuator–sensor system presents the use of three piezoelectric stack actuators placed in series to achieve the desired maximum stroke, several discrete strokes, an improved stroke resolution, and the ability to sense the actuator behaviour. The idea is to combine the piezo and inverse piezo effect, thus achieving the functionality of the actuator–sensor system. As noted in [19], the partially failed piezoelectric stack actuators may have a major impact on actuator performance and can be detected during the operation by monitoring their static and dynamic behaviour. The concept, shown in Figure 4a, is employed as a piezoelectric actuator–sensor system in hydraulic on/off valves integrated into a four-way digital fluid control unit (4WDFCU). The piezoelectric actuator system assembly, as shown in Figure 4b and its real picture in Figure 4c, consists of the following components: (1) a screw cap that provides a proper preload for the piezo stacks, (2) a spacer combined with a ball bearing to eliminate torsion, (3) an actuator housing, (4) a flange for installation in the hydraulic valve, (5) disc springs, and (6) a control piston and piezo element (PE). All the main steel parts of the actuator system (components 1, 2, 3, and 6) have been analyzed using the finite element method (FEM) to ensure the construction achieves a longitudinal deformation of less than one micron during operation.

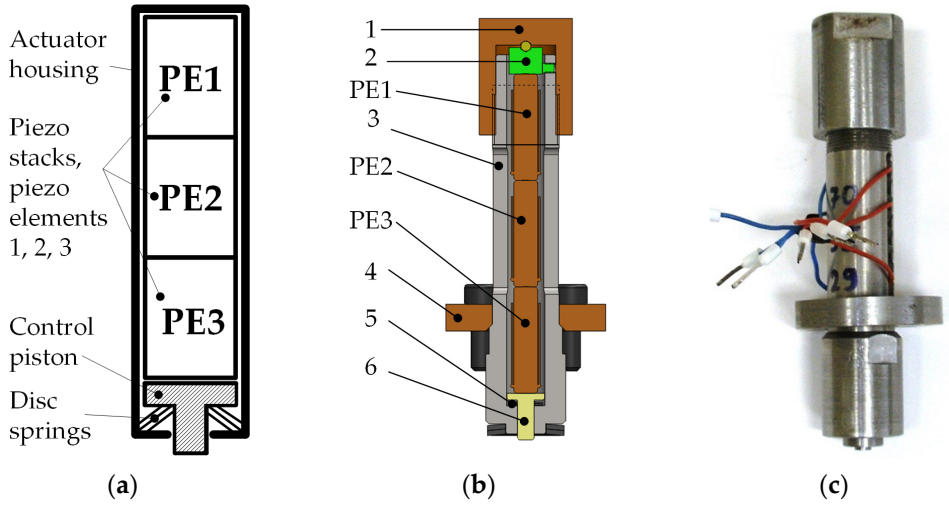

Figure 4. Concept of piezoelectric actuator system (**a**), cross-section view of serial-connected piezo elements (PE) (**b**), and real picture of piezoelectric actuator system (**c**).

The actuator housing, combined with disc springs and a control piston, facilitates the proper installation of the piezo elements. Using three piezoelectric elements (PEs) within a single actuator system allows for at least three discrete actuator stroke values, which is crucial for managing production costs and ensuring a high response rate when charging individual PEs. As mentioned, the non-activated PEs serve as sensors to monitor the PEs and the actuator system by measuring the electric voltage, which results from the extension of the active PEs and the generated force acting as an external load on the non-activated PEs. Digital fluid control units typically consist of multiple on/off valves arranged in parallel, meaning several valves and actuators must be used to achieve multiple discrete output values (in the case of hydraulic actuators, the output value is the actuator stroke, which directly corresponds to the valve flow rate).

The main characteristics of the piezoelectric stack actuator used in this investigation are presented in Table 1. It is made from SONOX P505 material and manufactured by CeramTec [14]. The key static performance characteristics include dimensions (cross-

section of 7 × 7 mm and effective height of 32.4 mm), the maximum free displacement (approximately 0.15% of the effective height), blocking force (2 kN), and the maximum control voltage (200 V). The actuator's dynamic performance is defined by its electrical capacitance and resonant frequency. The preload for the piezoelectric stack actuator is achieved using the screw cap, as shown in Figure 4b, position 1.

Table 1. Characteristics of piezoelectric stack actuator used in experimental investigation [14].

Characteristic	Value/Type
Dimensions (cross-section///height) [mm]	7 × 7///32.4
x_{free}, free displacement [microns]	46.70
F_{block}, blocking force [kN]	2.00
C, electrical capacitance [µF]	2.28
f_{res}, resonant frequency [kHz]	37.30
U_{max}, maximal control voltage [V]	200.00

The second important component of the piezoelectric actuator system is the disc spring unit, which provides the necessary initial preload for the piezoelectric elements (PEs). The disc spring unit deflects when the PEs are activated, as shown in Figure 4b, position 5. Table 2 presents the theoretical characteristics of a single disc spring (Value 1) and the measured characteristics of the disc spring unit (Value 2) used in the piezoelectric actuator system [20]. Three single disc springs are arranged in series to achieve the appropriate stiffness for the disc spring unit. The assembly of the disc springs was conducted under dry conditions (cleaned and dried discs) with no lubrication added between the discs. A total of 20 measurement cycles were performed for each characteristic point, with the standard deviation not exceeding 3%. Based on the data in Table 2 (Value 2), we can define four stiffness regions by calculating the stiffnesses of the disc spring unit. Since the disc spring unit was tested rather than calculated based on a single disc spring, friction and contact behaviour between the discs were taken into account. The results indicate an approximate 1.5% increase in force due to internal friction or other material losses.

Table 2. Characteristics of single disc spring.

Characteristic	Value 1 [20]	Value 2
Dimension [mm]	10 × 5.2 × 0.5	
Deflection 1 [mm]///Force 1 [N]	0.06///122	0.06///372
Deflection 2 [mm]///Force 2 [N]	0.13///228	0.13///694
Deflection 3 [mm]///Force 3 [N]	0.19///325	0.19///989
Deflection 4 [mm]///Force 4 [N]	0.25///418	0.25///1272

Alongside the extension of the piezoelectric elements (PEs), the disc springs are preloaded during installation and deflected during the operation of the piezoelectric actuator system. Based on the deflection–force relationship provided in Table 2 and additional testing of the disc spring unit, the actual disc spring stiffness was determined. Since the disc spring unit is preloaded, the piezoelectric actuator system operates primarily in Area 3, as shown in Figure 5. This figure illustrates the theoretical stroke of the piezoelectric actuator system, considering the characteristics of the PEs (three PEs in series) and the disc spring unit. The deformation of the piezoelectric actuator unit housing is ignored. The initial preload of the piezoelectric actuator system is F_{konst} = 620 N, resulting in an initial deflection of the disc spring unit of $x_{DS,\,konst}$ = 115 microns. The starting point S_p represents the initial condition of the piezoelectric actuator system. We considered a simplified theoretical model (as given by Equation (8) and graphically shown in Figure 3). The piezoelectric actuator system begins to extend under the applied electrical voltage, resulting in an actuator system stroke x_{pa}. Simultaneously, the generated force of the PEs F_{pa} decreases from the initial blocking force of 2 kN to approximately 980 N. Consequently, the disc spring unit is further

deflected by Δx_{DS}. The operating point (OP) indicates the maximum theoretical stroke of the piezoelectric actuator system, with x_{pa} being approximately 72 microns.

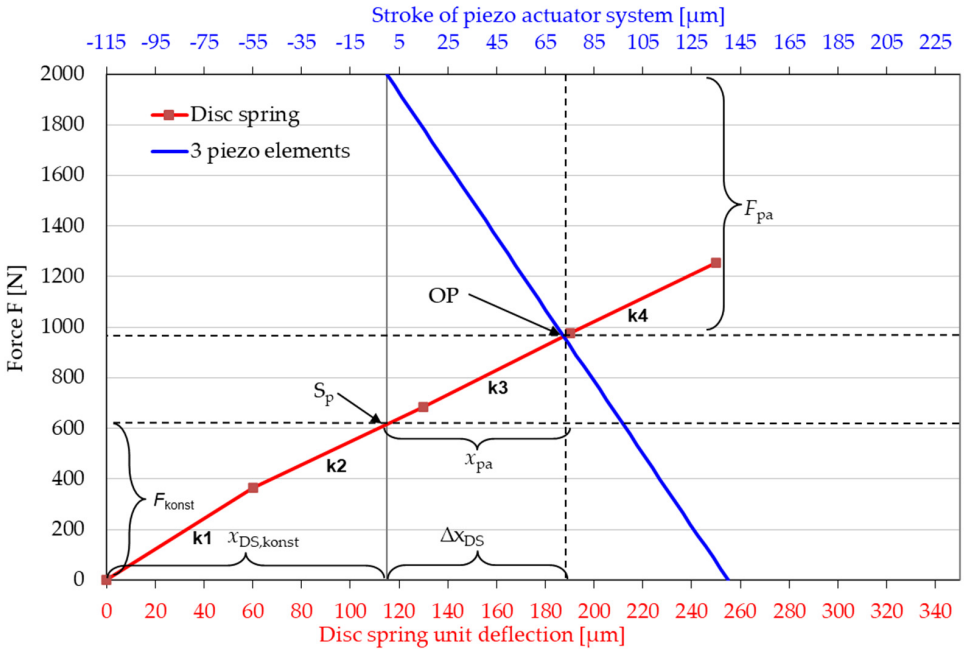

Figure 5. Theoretical stroke of piezo actuator system considering the disc spring stiffness.

4. Experimental Setup and Methodology

4.1. Test Rig Setup

In this section, the experimental setup and measurement methods for characterizing the piezoelectric actuator system are described. Both static and dynamic characteristics are presented in detail, which are crucial for switching technology and for open-loop as well as closed-loop position control. Two main parameters are measured and analyzed, (1) the stroke, or displacement, of the piezoelectric actuator system (x_{pa}) and (2) the electrical voltage applied to each piezo stack actuator (U_{PE1}, U_{PE2}, U_{PE3}).

The experimental setup is illustrated in Figure 6, with a real picture of the test rig shown in Figure 7. A personal computer with NI LabVIEW programming and a graphical user interface was employed to conduct test cycles, manage open-loop position control, monitor measured variables, and save the results. Standard block diagrams and the NI LabVIEW library were used to create all functional diagrams. The BNC-2120 external terminal (DAQ—data acquisition device) from National Instruments was used to capture the measured variables, including the stroke of the piezoelectric actuator system (measured by an Eddy current sensor) and the electrical voltage at each PE. This device can acquire both analogue and digital signals and is compatible with NI LabVIEW, allowing for the setting of data types, sampling frequency, and triggers. It supports high-frequency data acquisition, ranging from 100 Hz to 1 MHz [21].

Pulse number modulation (PNM) was utilized for open-loop position control to determine the three discrete values of the piezoelectric actuator system's stroke (with one, two, or three PEs activated). Custom digital control electronics, including low-voltage high-response switching electronics and high-voltage control electronics, have been developed to achieve high response rates, high voltage signals, and stable control. The PNM method employs standard on/off pulses (low-voltage electronics with 5 V pulses to control high-voltage switches producing a 200 V output control pulse signal—$U_{S,PEi}$).

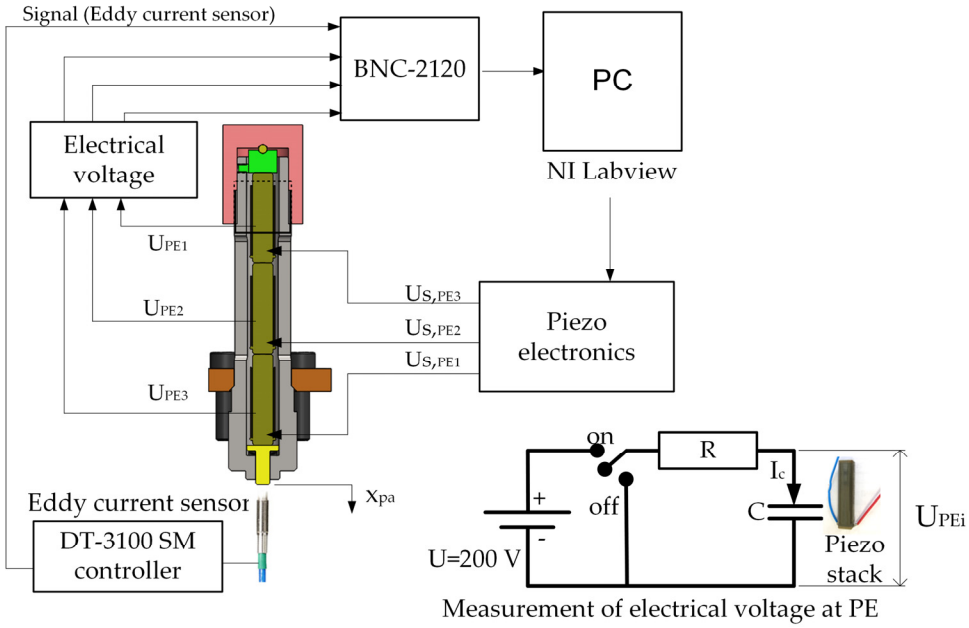

Figure 6. Scheme of experimental setup and measured voltage at each PE.

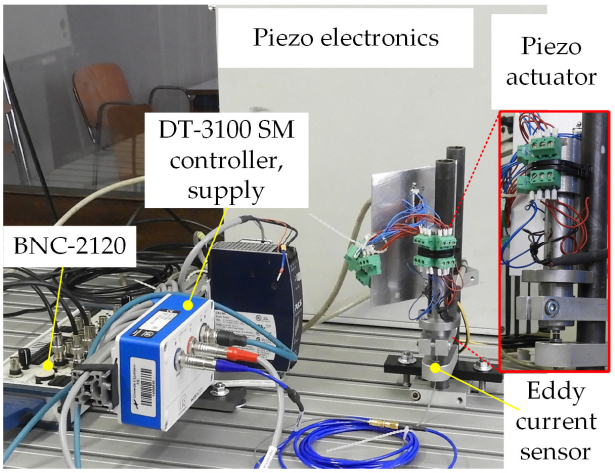

Figure 7. Real picture of experimental test rig.

Additionally, the pulse width modulation (PWM) method was combined with closed-loop position control using a PID controller and a position sensor in the feedback loop. The desired position of the piezoelectric actuator system was used as the reference signal [22]. For PWM, the parameters were set at the low-voltage electronics (5 V output signals) with a frequency of 100 Hz, resulting in 100 signals per second. The duty cycle varied from 10% to 100% depending on the required signal in the closed-loop control. A period of 10 microseconds was used, with a linear step response set to 0.1 milliseconds for rise and fall times. Based on the static characteristics of the piezoelectric actuator system, the control activated one, two, or three PEs for a specified time period to achieve the desired stroke. Only the proportional (P) gain was used in the high-voltage control electronics (amplifier) to achieve the desired step response and fast charging of the PEs. The P gain was set to 30, while the integral (I) and derivative (D) gains were set to zero or excluded from the closed-loop control.

The overall displacement of the piezoelectric actuator system (stroke) was measured using the Micro-Epsilon U1 eddy current sensor, which has a measuring range of up to 1 mm and a stroke resolution of less than 0.1 microns. Calibration was performed using the Micro-Epsilon online tool. To accurately capture signals from the eddy current sensor, the

DT 3100 SM controller, equipped with an integrated amplifier and null shift function, was used. The extension of the piezoelectric stack actuator is indirectly influenced by the supply voltage ($U_{s,PEi}$). Therefore, the electrical voltage at each piezo stack (U_{PEi}) was measured to facilitate a more in-depth analysis. Since the system operated in different scenarios, with one, two, or three PEs active at a time, we anticipated measuring electrical voltage at inactive PEs due to the force generated by the active PEs affecting the entire piezoelectric actuator system.

4.2. Static and Dynamic Characteristics' Measurement

The static characteristics include piezoelectric actuator system stroke x_{pa} for several different operating scenarios (one active PE, two active PEs, and three active PEs) at the maximum control voltage $U_{S,PEi}$ = 200 V. The PNM method is used here to simplify control. We expected at least three discrete stroke values for the piezoelectric actuator system. Three scenarios were presented for activating a single PE (PE1, PE2, or PE3), as shown in Figure 8a. Similarly, three scenarios were planned for activating two PEs (PE1 + PE2, PE1 + PE3, and PE2 + PE3), as illustrated in Figure 8b. The final scenario involved activating all three PEs, as depicted in Figure 8c. For a better understanding, the voltage measured at each piezoelectric stack actuator was analyzed, which is directly measured at the positive and negative poles of the PEs (Figure 6).

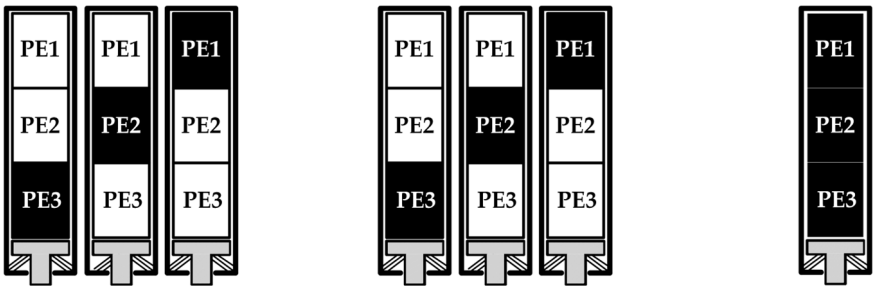

Figure 8. Control scenarios. one active PE (**a**), two active PEs (**b**) and three active PEs (**c**).

The static characteristics, particularly the potential for a higher stroke resolution of the piezoelectric actuator system, were analyzed using the PWM method. The width of the PWM control signal determines how long the PE remains activated. Since the PE requires a certain amount of time to reach full extension, low-width PWM signals can be used to achieve a partially extended PE, resulting in the partial displacement of the piezoelectric actuator system.

The dynamic characteristics include the step response of the piezoelectric actuator system. Theoretically, the piezoelectric stack actuator (PE) can be modeled as an RC electrical circuit, as presented in [22] and shown schematically in Figure 6. In this case, the charging curve represents the response of a first-order system. Additionally, since the piezoelectric actuator system operates as a mechanical system (a mass–spring–damper system), the step response can be characterized as a second-order system, as defined by Equation (9) [23].

$$m_s \cdot \ddot{x}_s(t) = F_s(t) - b_s \cdot \dot{x}_s(t) - k_s \cdot x_s(t) \quad (9)$$

where m_s represents the effective mass of the moveable parts, F_s denotes the induced (or generated) force, b_s is the damping coefficient of the system, and k_s represents the stiffness of the system.

The second-order system response is graphically shown in Figure 9. The x-axis represents time and the y-axis denotes the amplitude, corresponding to the piezoelectric actuator system stroke (response). The transient response of a practical system often displays damped oscillations before reaching a steady state. The response curve is characterized by several key parameters, namely the rise time t_r (time taken to rise from 10% to 90% of the

final value), the peak time t_p (time required for the response to reach the first peak of the overshoot), and the settling time t_s (time taken for the response to settle within its specified tolerance, which in our case is ±2%). The response also exhibits a typical peak overshoot A, along with a steady-state error e [23].

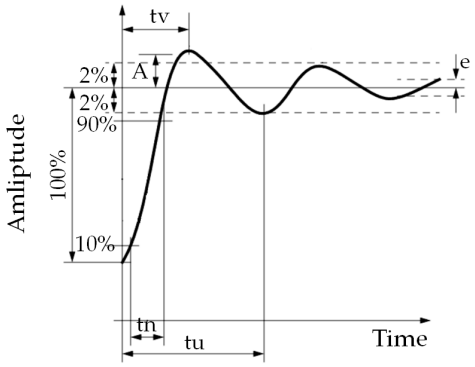

Figure 9. Step response of a second-order system.

In this paper, the step response time is defined by the rise time t_n, which corresponds to the piezoelectric actuator system stroke increasing from 10% to 90% of its amplitude value [23]. Our aim is to achieve a step response for the piezoelectric actuator system without overshoot, stable conditions without oscillations, and a minimal steady-state error of less than 1 micron.

5. Results and Discussion

A detailed experimental analysis was conducted to examine the static and dynamic characteristics of the piezoelectric actuator system. The static characteristics include determining the actuator stroke under various operating scenarios and measuring the electrical voltage at each PE to characterize piezo behaviour, specifically the electrical voltage curve for both active and inactive PEs. The final test demonstrates the potential stroke resolution of the piezoelectric actuator using the PWM control strategy. The dynamic analysis focuses on determining the step response of the piezoelectric actuator system under different control strategies.

5.1. Static Performance of Piezoelectric Actuator System

The first discrete value of the piezoelectric actuator system stroke, x_{pa}, is achieved by activating a single PE (Table 3 and Figure 10, Case 1—activation of PE1, PE2, or PE3). In all three scenarios, the average stroke is 29.3 microns (at steady state), with no significant effect under which PE is activated. Based on 10 tests for each PE, the standard deviation of the piezoelectric actuator stroke remains within 1%. Activating two PEs (Table 3 and Figure 10, Case 2) results in an average stroke of 52.7 microns, while activating all three PEs (Table 3 and Figure 10, Case 3) yields an average stroke of 71.2 microns. The actuator stroke is noticeably smaller than the free displacement of an individual PE (x_{free} = 46.7 µm). According to the variable load applied to the piezoelectric stack actuator and the operating principle presented in Figure 3 and Equation (8), these results are expected and align with the theoretical curve shown in Figure 5. The actuator system displacement (stroke) decreases linearly as preload increases. Additionally, the minor contraction of inactive PEs, caused by their stiffness (less than one micron per PE), contributes to the overall reduction. Inactive PEs act as elastic bodies with a high stiffness affected by the external load generated by the active PE.

The piezo effect, used in sensor technology, is clearly demonstrated by analyzing the electrical voltage curves shown in Figure 11. Seven different combinations of active piezo stacks are analyzed in detail.

Table 3. The stroke depended on the number of active PEs.

Active State	Actuator Stroke x_{pa} [µm]
Case 1—one active PE	29.3
Case 2—two active PEs	52.7
Case 3—three active PEs	71.2

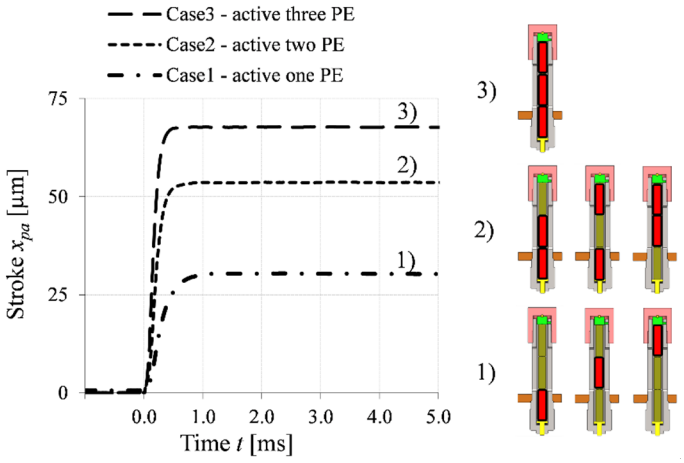

Figure 10. Maximum stroke of piezoelectric actuator system vs. active PE.

The first three scenarios, presented in Figure 11a–c, show one active PE. The high electrical voltage overshoot observed on PE2 (Figure 11a, UPE2) can be attributed to its proximity to the active PE3, where it is influenced by the high axial force generated by the actuator system's response. Activating PE2 or PE3 results in a lower electrical voltage overshoot at the inactive PE1. This can be explained by the fact that PE2 affects both PE1 and PE3, distributing the generated force between them. The maximum electrical voltage measured at the inactive PEs remains consistent across all three scenarios, at around 80 ± 5 V. Similar explanations apply to other scenarios where two or three PEs are activated. When two PEs are active, shown in Figure 11d–f, the measured electrical voltage is higher, around 100 ± 5 V in the stationary state. This is because two active PEs provide a greater stroke of the piezoelectric actuator system (greater extension of PEs), resulting in a higher pretension in the disc spring unit and consequently, a higher axial force acting on the system. A detailed analysis of the three-active-PE scenario reveals two regions of electrical voltage increase. The first region shows an increase in voltage up to 100–120 V, followed by a decrease. The second region represents an additional voltage increase up to the maximum value of 200 V. We believe this intermediate phenomenon is due to the high generated piezo force (blocking force) observed at the beginning of piezo actuator activation before the extension begins.

With the appropriate piezo electronics and a combination of pulse number modulation (PNM) and pulse width modulation (PWM), the number of discrete values for the piezoelectric actuator system stroke can be increased. Operating with a base signal width of 10 µs allows us to create a 5 V control signal ranging from 10 µs to 1000 µs, with increments of 10 µs. The PWM signal width directly affects the activation of high-response switches in the high-voltage electronics, thereby increasing the control voltage applied to the piezo stacks. A minimal actuator stroke, approximately 1.5 microns, can be achieved using one piezo stack with a PWM signal width of 20 µs. Although the piezo electronics allow for a minimal PWM signal width of 10 µs, no actuator response is observed due to the generated force being insufficient to overcome the initial spring preload. Discrete values of the piezoelectric actuator system stroke for different PWM signals and the activation of one PE are shown in Figure 12a. Figure 12b illustrates the PWM signal at the low-voltage control electronics for a 100 µs width signal, resulting in a 20 µm piezoelectric actuator system stroke.

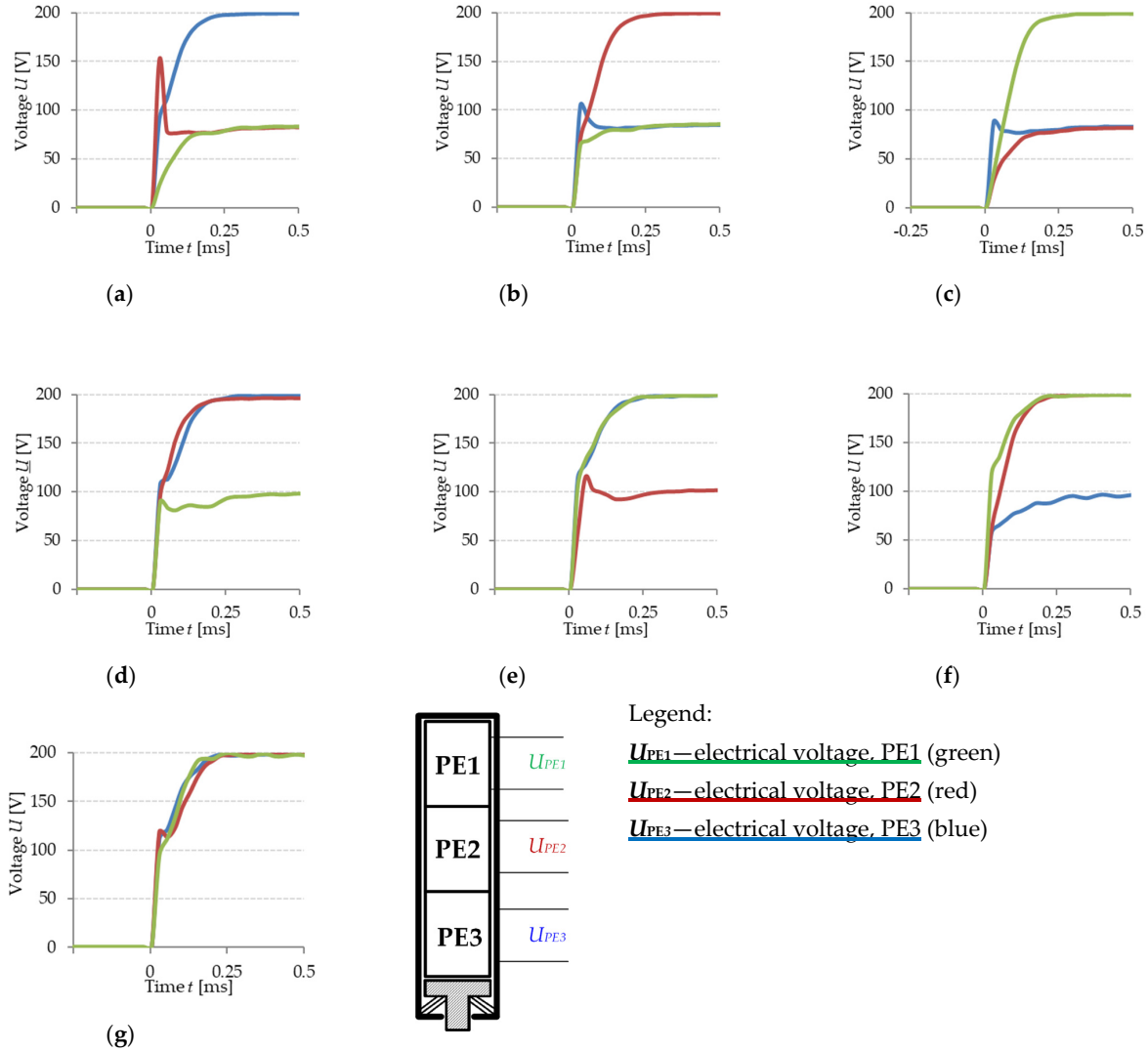

Figure 11. Electrical voltage measured on an individual PE when activating PE3 (**a**), PE2 (**b**), PE1 (**c**), PE2 and PE3 (**d**), PE1 and PE3 (**e**), PE1 and PE2 (**f**), and PE1, PE2, and PE3 (**g**).

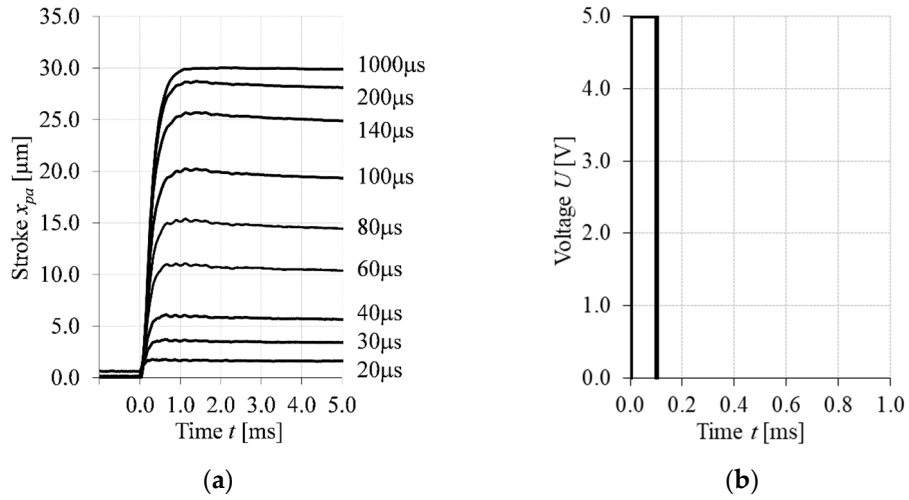

Figure 12. Discrete values of PE stroke achieved with the PWM control strategy (**a**) and a control signal of 0.1 ms to achieve a 20 µm piezo electric actuator stroke (**b**).

5.2. Dynamic Performance of Piezoelectric Actuator System

The step response of the piezoelectric actuator system is represented by the time t_n in Table 4 and is graphically shown in Figure 13. Case 1 presents the activation of one PE, Case 2 the activation of two PEs, and Case 3 the activation of three PEs. A detailed analysis shows different response times for these scenarios. The shortest response time, t_{n3} = 0.185 ms, is achieved by activating all three PEs. This can be attributed to the higher stiffness of the active PEs compared to the inactive ones, resulting in a stiffer overall piezoelectric actuator system. Conversely, the longest response time, t_{n1} = 0.450 ms, occurs when only one PE is activated. This longer response time is due to energy losses associated with acting on non-active PEs with the generated force. Activating two PEs results in a step response time of t_{n2} = 0.280 ms, reflecting intermediate conditions between the one-PE and three-PE scenarios.

Table 4. The step response of the piezoelectric actuator system depended on the control strategy.

Active State	t_n [ms]
Case 1—one active PE	0.450
Case 2—two active PEs	0.280
Case 3—three active PEs	0.185

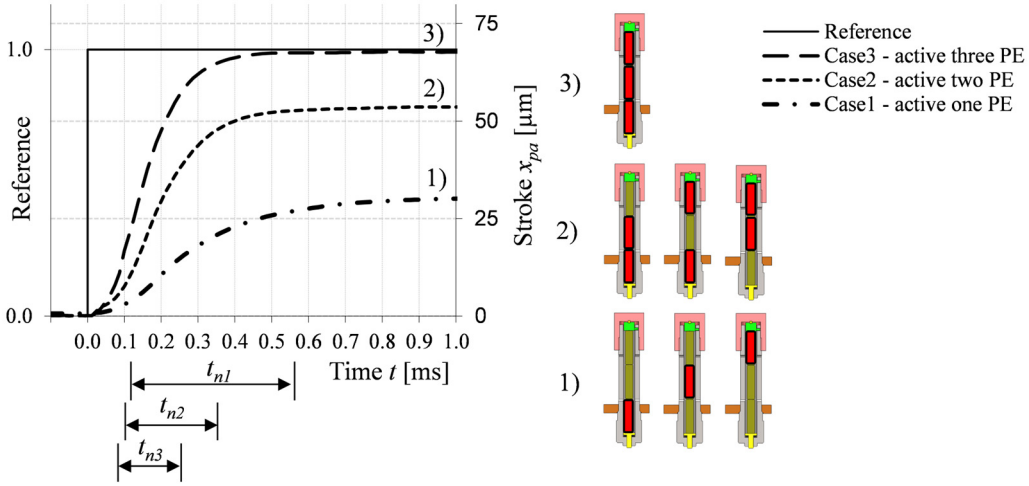

Figure 13. The step response of the piezoelectric actuator system depended on active PEs.

Considering the activation of one PE and using PWM control to achieve different discrete values of the piezoelectric actuator system stroke (Figure 13), the step response time varies from 0.15 ms to 0.45 ms. A detailed view of activating one PE with different PWM signal widths, ranging from 20 µs to 1000 µs, is shown in Figure 14a. Additionally, the step response for a PWM signal width of 20 µs is illustrated in Figure 14b.

The step response of the piezoelectric actuator system can be significantly improved by using a boosting control strategy (Figure 15, Case 4), which involves activating all three PEs simultaneously with the maximum electrical voltage U = 200 V. Similar techniques were used for on/off switching solenoid valves, where the maximum supply voltage (control signal) was used at the beginning of the activation cycle and followed by a proper low-voltage signal to remain in the active state of the actuator [24,25]. This approach achieves a high step response across different strokes, with a response time of approximately 0.25 ms. Compared to other commercially available piezoelectric stack actuators, our design demonstrates equal or potentially superior dynamic performance. For example, according to their technical specifications, the P-810/30, P-840, and P-841 models from Physik Instrumente exhibit sub-millisecond response times [11]. Similarly, Cedrat Technologies' parallel pre-stressed piezo actuators of type PPA40L show a step response time of around 0.15–0.25 ms, which is comparable to our actuator's performance [26].

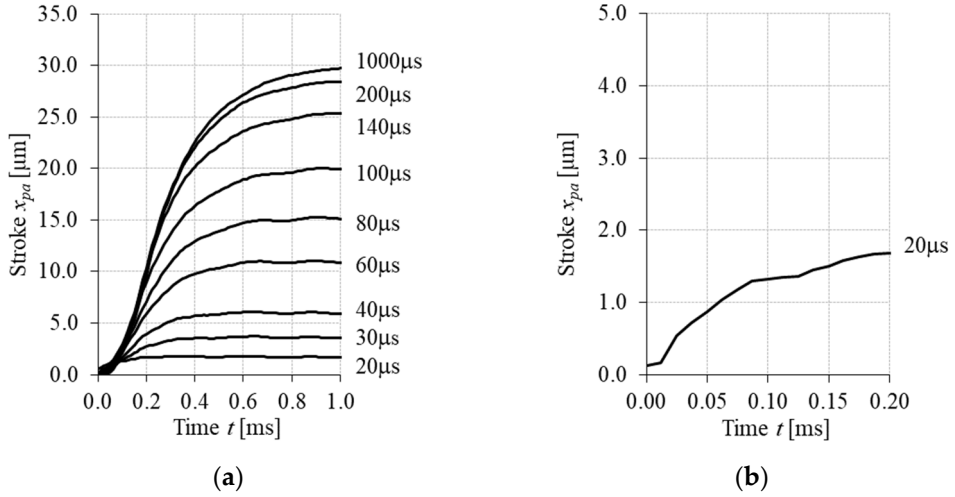

Figure 14. Step response of the piezoelectric actuator system with one PE using PWM control. Overview with varying PWM signal widths (**a**) and detailed view with a 20 µs PWM signal (**b**).

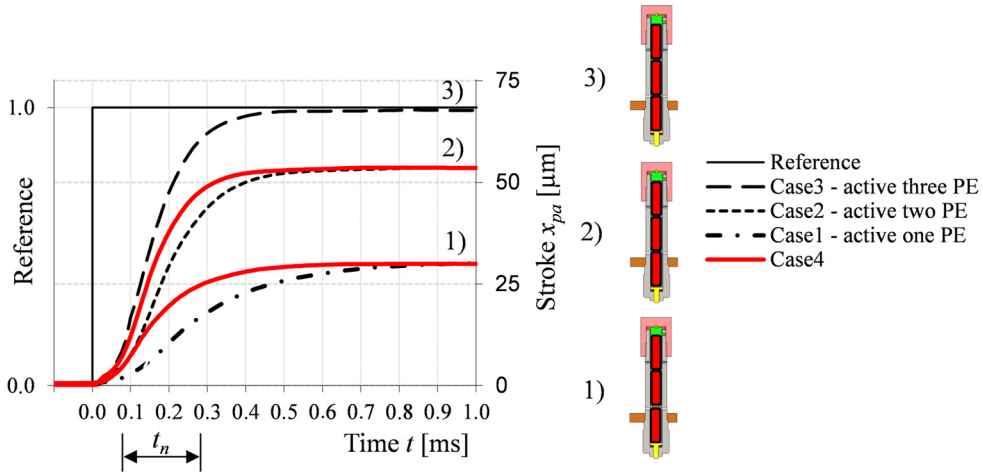

Figure 15. Improved step response of the piezoelectric actuator system.

The desired discrete values of the piezoelectric actuator stroke are achieved by activating the PEs for specific durations. Experimental tests show that a 30 µm stroke is obtained by activating all three PEs for 60 µs. Similarly, a 52 µm stroke is achieved with a 90 µs activation, and a 71 µm stroke requires 130 µs of activation. The use of multiple piezoelectric stack actuators (PEs) in series, rather than a single 90 mm actuator, is crucial. Longer PEs have a higher electrical capacitance (*C*), which results in longer charging times to achieve the desired displacement. To address this, new piezo electronics have been developed to control each PE independently. Each PE is equipped with its own low-voltage and high-voltage amplifier, as well as a capacitor for energy storage. This setup allows for the simultaneous high-potential activation of the PEs, enabling faster charging due to the low electrical capacitance of the stack actuators. This approach is particularly useful when achieving a rapid step response is more critical than high accuracy in the piezoelectric actuator system.

5.3. Concept of Smart Piezoelectric Actuator System

Figure 16 illustrates the potential application of piezoelectric actuator systems in a four-way digital fluid control unit (4WDFCU) for both the open-loop and closed-loop position control of hydraulic drives. The system uses four piezo valves to replicate the functionality of a four-way, three-stage conventional spool valve. The 4WDFCU features a modular design, allowing for the replacement of piezo valves and actuator systems. This

flexibility enables the configuration of the 4WDFCU to meet specific hydraulic application requirements, optimizing both static and dynamic performance. Additionally, the integration of wireless 5G technology and RFID is proposed to enable efficient plug-and-play functionality and facilitate data transfer between the actuator, valve, and controller unit [27].

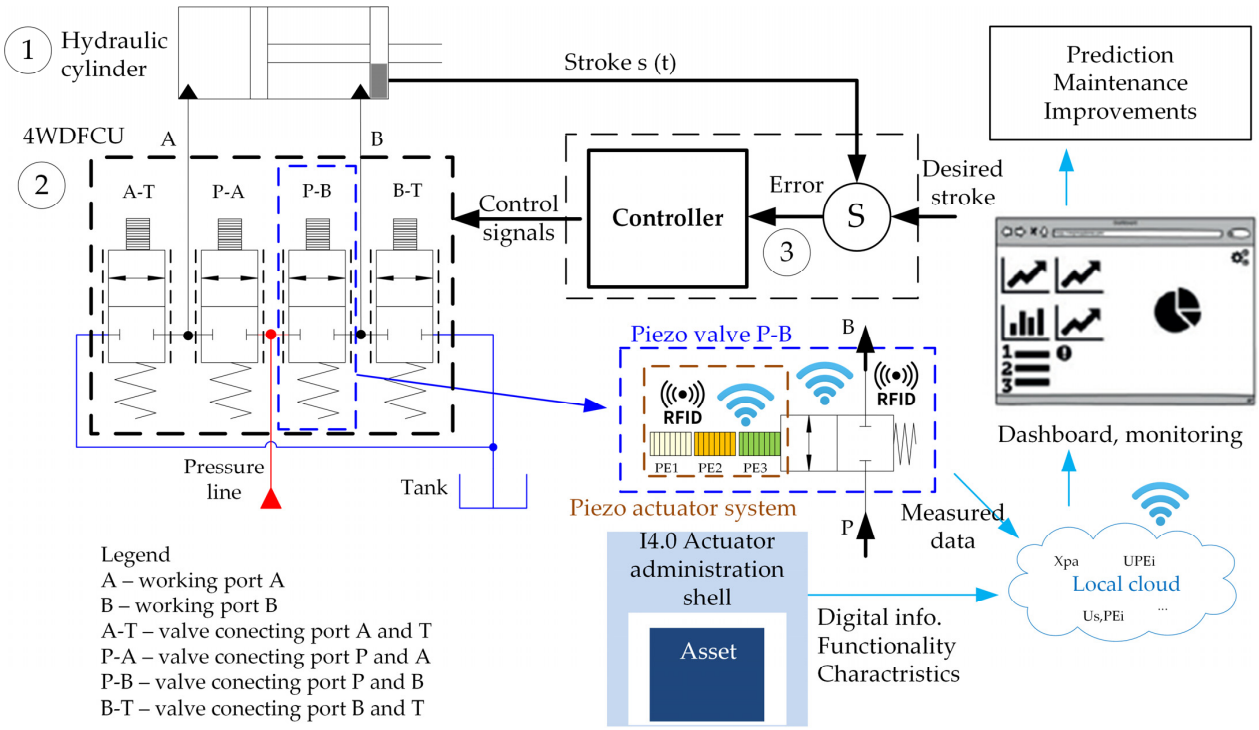

Figure 16. The concept of smart piezoelectric actuators used in hydraulic on/off valves and the integrated Asset Administration Shell.

The Asset Administration Shell (AAS) concept is proposed for use with piezoelectric actuator systems and hydraulic valves. The AAS is a data and information model employed in the Industrial Internet of Things (IIoT) to describe and manage assets. Essentially, the AAS acts as a data plug, enabling the retrieval and storage of all relevant information about a specific asset, device, or component [28]. In this context, the AAS will facilitate efficient connectivity, asset recognition, and data transfer between the piezoelectric actuator system and the valve. This integration will allow for automatic adaptation and parameter setup according to the hydraulic drive application, optimizing the performance of hydraulic components.

Additionally, real-time data from the piezoelectric actuator system and hydraulic valve can be stored on a local cloud for future use, such as edge computing. These data will enable real-time monitoring to assess component health, static and dynamic performance, energy consumption, and more. It will also be accessible to component developers and manufacturers to predict and implement potential improvements in design or setup.

6. Conclusions

This paper presents a new piezoelectric actuator system design and its static and dynamic characteristics, which can be included into the Actuator Administration Shell. The system is used in hydraulic on/off valves integrated into four-way digital fluid control units (4WDFCUs). The design includes three piezo stack actuators in series, achieving actuator–sensor capabilities. Each actuator has a free displacement of 46 µm, a blocking force of 2 kN, and is preloaded with 620 N. Two control methods are used, pulse number modulation and pulse width modulation, providing discrete displacement values of 29.3 µm (one PE),

52.7 µm (two PEs), and 71.2 µm (three PEs). Inactive piezo stacks act as sensors due to the axial force generated from active piezo stacks. PWM allows for finer control, with a minimum stroke of 1.5 µm. Activating one PE gives a step response time of 0.450 ms, while three PEs result in 0.185 ms. Using PWM with all three PEs stabilizes the response at around 0.2 ms.

Author Contributions: Conceptualization, methodology, software, formal analysis, investigation, resources, data curation, writing—original draft preparation, M.Š.; validation, M.Š. and N.H.; writing—review and editing, visualization, supervision, project administration, funding acquisition, N.H. All authors have read and agreed to the published version of the manuscript.

Funding: This research was funded by the Slovenian Research and Innovation Agency—ARIS, research project Research on the reliability and efficiency of edge computing in the smart factory using 5G technologies (funding number J2-4470) and research programme Innovative Manufacturing Systems and processes (funding number P2-0248), which are financed by the Republic of Slovenia—Ministry of Education, Science and Sport. The APC was funded by Slovenian Research and Innovation Agency—ARIS, research project Research on the reliability and efficiency of edge computing in the smart factory using 5G technologies, funding number J2-4470.

Institutional Review Board Statement: Not applicable.

Informed Consent Statement: Not applicable.

Data Availability Statement: The data are available within the article.

Conflicts of Interest: The authors declare no conflict of interest.

References

1. Ikpe, A.E.; Ekanem, I.I. Integration of Intelligent Hydraulic Systems as Industry 4.0 Driving Trends: The Gateway to Industrial Automation in The Manufacturing Sectors. In Proceedings of the EL RUHA 11. International Conference on Scientific Research, Sanliurfa, Turkey, 7–9 February 2024; pp. 255–276.
2. Herakovič, N.; Zupan, H.; Pipan, M.; Protner, J.; Šimic, M. Distributed manufacturing systems with digital agents. *Stroj. Vestn./J. Mech. Eng.* **2019**, *65*, 650–657. [CrossRef]
3. Sciatti, F.; Tamburrano, P.; Distaso, E.; Amirante, R. Digital hydraulic valves: Advancements in research. *Heliyon* **2024**, *10*, e27264. [CrossRef] [PubMed]
4. Šimic, M.; Herakovič, N. Characterization of energy consumption of new piezo actuator system used for hydraulic on/off valves. *J. Clean. Prod.* **2021**, *284*, 124748. [CrossRef]
5. Tic, V.; Ratovnik, A.; Lovrec, D. Impact of Proportional Valves' Differences to Ensure Uniform Motion of Hydraulic Motors. *Int. J. Simul. Model.* **2021**, *20*, 52–63. [CrossRef]
6. Topçu, E.; Yüksel, I.; Kamý, Z. Development of electro-pneumatic fast switching valve and investigation of its characteristics. *Mechatronics* **2006**, *6*, 365–378. [CrossRef]
7. Choi, S.B.; Yoo, J.K.; Cho, M.S.; Lee, Y.S. Position control of a cylinder system using a piezoactuator-driven pump. *Mechatronics* **2005**, *2*, 239–249. [CrossRef]
8. Choi, S.B.; Han, S.S.; Lee, Y.S. Fine motion control of a moving stage using a piezoactuator associated with a displacement amplifier. *Smart Mater. Struct.* **2005**, *1*, 222–230. [CrossRef]
9. Miyajima, T.; Fujita, T.; Sakaki, K.; Kawashima, K.; Kagawa, T. Development of a digital control system for high-performance pneumatic servo valve. *Precis. Eng.* **2007**, *2*, 156–161. [CrossRef]
10. Zhou, X.; Wu, S.; Wang, X.; Wang, Z.; Zhu, Q.; Sun, J.; Huang, P.; Wang, X.; Huang, W.; Lu, Q. Review on piezoelectric actuators: Materials, classifications, applications, and recent trends. *Front. Mech. Eng.* **2024**, *19*, 6. [CrossRef]
11. Physik Instrumente. Fundamentals of Piezo Technology. Available online: https://www.physikinstrumente.com/en/expertise/technology/piezo-technology/fundamentals (accessed on 16 September 2024).
12. Šimic, M.; Herakovič, N. Piezo actuators for the use in hydraulic and pneumatic valves. In Proceedings of the International Conference Fluid Power 2017, Maribor, Slovenia, 14–15 September 2024.
13. Gao, X.; Yang, J.; Wu, J.; Xin, X.; Li, Z.; Yuan, X.; Shen, X.; Dong, S. Piezoelectric Actuators and Motors: Materials, Designs, and Applications. *Adv. Mater. Technol.* **2020**, *5*, 1900716. [CrossRef]
14. CeramTec GmbH. Technical Specification of Piezo Ceramics and Piezo Actuators for Industrial Applications. CeramTec-Platz1–9, 73207 Plochingen, Germany. Available online: https://www.ceramtec-group.com/en/ (accessed on 1 July 2020).
15. Nasser, K.M. *Development and Analysis of the Lumped Parameter Model of a PiezoHydarulic Actuator*; Virginia Tech: Blacksburg, VA, USA, 2000.

16. Li, P.; Fu, J.; Wang, Y.; Xing, Z.; Yu, M. Dynamic model and parameters identification of piezoelectric stack actuators. In Proceedings of the 26th Chinese Control and Decision Conference (2014 CCDC), Changsha, China, 31 May–2 June 2014; pp. 1918–1923.
17. Stamatellou, A.M. PZT and PVDF piezoelectric transducers' design implications on their efficiency and energy harvesting potential. *Energy Harvest. Syst.* **2023**, *10*, 157–167. [CrossRef]
18. Sherrit, S.; Jones, J.M.; Aldrich, J.B.; Blodget, C.; Bao, X.; Badescu, M.; Bar-Cohen, Y. Multilayer piezoelectric stack actuator characterization. In *Behavior and Mechanics of Multifunctional and Composite Materials, Proceedings of SPIE Smart Structures and Materials + Nondestructive Evaluation and Health Monitoring, San Diego, CA, USA, 10–13 March 2008*; SPIE-International Society for Optics and Photonics: Bellingham, WA, USA, 2014; Volume 6929.
19. Yang, J.; Mao, Y.; Qu, B.; Yan, X.; Yang, M.; Zhou, B.; Lu, Y. Dynamic responses of normal and partially failed piezoelectric stack actuators under sinusoidal voltages with DC biasing. *Smart Mater. Struct.* **2024**, *33*, 095004. [CrossRef]
20. Hennlich. Technical Specifications—Disc Springs. Hennlich d.o.o., Ul. Mirka Vadnova 13, 4000 Kranj, Slovenia. Available online: http://www.hennlich.si/proizvodi/vzmetenje-kroznikaste-vzmeti-157/kroznikaste-vzmeti-iz-vzmetnega-jekla.html (accessed on 1 July 2020).
21. National Instruments. Installation Guide BNC-2120 Connector Accessory for E/M/S/X Series Devices, NI LabVIEW. National Instruments Corporation. Available online: https://www.ni.com/en.html (accessed on 21 February 2023).
22. Kanchan, M.; Santhya, M.; Bhat, R.; Naik, N. Application of Modeling and Control Approaches of Piezoelectric Actuators: A Review. *Technologies* **2023**, *11*, 155. [CrossRef]
23. Podržaj, P. *Linear Theory of Control Systems*; University of Ljubljana, Facility of Mechanical Engineering: Ljubljana, Slovenia, 2021; p. 208, ISBN 978-961-6536-49-3.
24. Zhao, J.H.; Wang, M.L.; Wang, Z.J.; Grekhov, L.; Qiu, T.; Ma, X.Z. Different Boost Voltage Effects on the Dynamic Response and Energy Losses of High-speed Solenoid Valves. *Appl. Therm. Eng.* **2017**, *123*, 1494–1503. [CrossRef]
25. Gao, Q.; Wang, J.; Zhu, Y.; Wang, J.; Wang, J. Research Status and Prospects of Control Strategies for High Speed On/Off Valves. *Processes* **2023**, *11*, 160. [CrossRef]
26. CEDRAT TECHNOLOGIES. Parallel Pre-stressed Actuator. Available online: https://cedrat-technologies.com/categorie-produit/piezo-actuators/amplified-piezo-and-parallel-pre-stressed/parallel-pre-stressed-actuator-piezo-actuators/ (accessed on 16 September 2024).
27. Rao, S.K.; Prasad, R. Impact of 5G Technologies on Industry 4.0. *Wirel. Pers. Commun.* **2018**, *100*, 145–159. [CrossRef]
28. Sakurada, L.; Leitao, P.; De la Prieta, F. Agent-Based Asset Administration Shell Approach for Digitizing Industrial Assets. *IFAC-PapersOnLine* **2022**, *55*, 193–198, ISSN 2405-8963. [CrossRef]

Disclaimer/Publisher's Note: The statements, opinions and data contained in all publications are solely those of the individual author(s) and contributor(s) and not of MDPI and/or the editor(s). MDPI and/or the editor(s) disclaim responsibility for any injury to people or property resulting from any ideas, methods, instructions or products referred to in the content.